Appl. Phys. A 69 [Suppl.], S783–S785 (1999) / Digital Object Identifier (DOI) 10.1007/s003399900231

Applied Physics A
Materials
Science & Processing
© Springer-Verlag 1999

Structural and electrical properties of $La_{0.5}Sr_{0.5}CoO_3$ films on $SrTiO_3$ and porous α-Al_2O_3 substrates

E.A.F. Span*, **F.J.G. Roesthuis, D.H.A. Blank, H. Rogalla**

Department of Applied Physics, University of Twente, P.O. Box 217, 7500 AE Enschede, The Netherlands

Received: 21 July 1999/Accepted: 31 August 1999/Published online: 22 December 1999

Abstract. Films of $La_{0.5}Sr_{0.5}CoO_3$ (LSCO) have been deposited on specially treated TiO_2-terminated (001) $SrTiO_3$ substrate surfaces and on macroporous polycrystalline α-Al_2O_3 substrates, having a mean pore diameter of 80 nm, by pulsed laser deposition. The films deposited on $SrTiO_3$ are good conducting, (001) textured, and exceptionally smooth (1–2 Å for 100 nm thick films). LSCO films deposited on porous α-Al_2O_3 are polycrystalline and exhibit good crystallographic and electrical properties despite the large substrate roughness and the differences in lattice parameters and crystal structure between the film and the substrate. Different growth modes have been observed on the porous α-Al_2O_3 substrates depending on the oxygen pressure during film deposition. Films grown at an oxygen pressure of 10^{-1} mbar are macroporous, whereas films grown at 10^{-2} mbar completely cover the substrate pores. In the latter case, strain effects lead to film cracking.

PACS: 81.15.Fg; 68.15.Jk; 81.05.Je

The pseudo-cubic perovskite $La_{0.5}Sr_{0.5}CoO_3$ (LSCO) exhibits a high electronic and oxygen ionic conductivity, good chemical stability, and high catalytic activity. Films of LSCO are therefore of great technological importance since they can be used for a wide range of applications. On the one hand, epitaxial LSCO films are studied for electronic applications like nonvolatile ferroelectric memory devices and high-T_c superconducting Josephson junctions [1–5]. On the other hand, epitaxial, polycrystalline, and porous films of LSCO and other related compounds from the (La, Sr)(Co, Fe)O_3 family are studied for application in various electrochemical devices like solid oxide fuel cells, oxygen separation membranes, and gas sensors [6–11]. So far, there have been no reports on the growth of LSCO on porous substrates by pulsed laser deposition. In this paper, we report on the properties of LSCO films deposited on macroporous α-Al_2O_3 substrates for electrochemical applications by pulsed laser deposition. For comparison, the properties of epitaxial LSCO films deposited on high- quality $SrTiO_3$ substrates are also discussed.

*Corresponding author.
(Fax: +31-53/4891099, E-mail: e.a.f.span@tn.utwente.nl)

COLA'99 – 5th International Conference on Laser Ablation, July 19–23, 1999 in Göttingen, Germany

1 Experimental

LSCO films were deposited from a rotating stoichiometric $La_{0.5}Sr_{0.5}CoO_3$ target (polycrystalline, 99% dense) by a 248 nm KrF excimer laser (Lambda Physik). The fluence used was 1.5 J/cm^2, which is well above the threshold for stoichiometric ablation [12]. The deposition temperature was varied between 500 and 800 °C. After growth, the films were annealed for 1 h in 1 bar oxygen pressure at the deposition temperature and subsequently cooled at a rate of 5 °C min^{-1} to room temperature. The films were deposited on specially treated, well-defined, TiO_2-terminated (001) $SrTiO_3$ substrates surfaces [13] as well as on round (∅15 mm), polycrystalline, macroporous α-Al_2O_3 substrates that were synthesized from commercially obtained powder. The mean pore diameter of these substrates as determined by mercury porosimetry is 80 nm. SEM and AFM were used to examine the film surface morphology and EDX was used to determine the average composition of the films. The film structure was analyzed by XRD and the film resistivity was measured by a standard four-point probe measurement.

2 Results and discussion

Stoichiometric and exceptionally smooth LSCO films were grown on $SrTiO_3$ in the temperature range 550–700 °C. The oxygen pressure during deposition and the target-to-substrate distance were kept constant at optimized values of 0.1 mbar and 63 mm, respectively. The repetition frequency was 5 Hz. The film resistivity was lowest for films grown at temperatures between 580–640 °C. In this temperature range, the

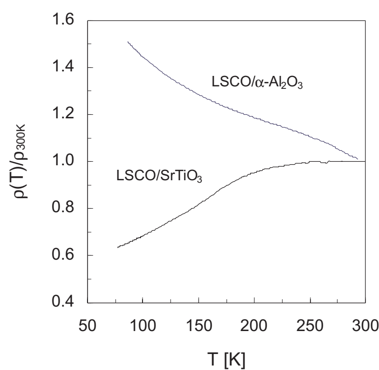

Fig. 1. Normalized temperature dependence of the electrical resistivity of a (001) textured LSCO/ $SrTiO_3$ film (deposition temperature 620 °C) and a polycrystalline LSCO/ α-Al_2O_3 film (deposition temperature 650 °C). Both films were grown at an oxygen pressure of 0.1 mbar and a target-to-substrate distance of 63 mm

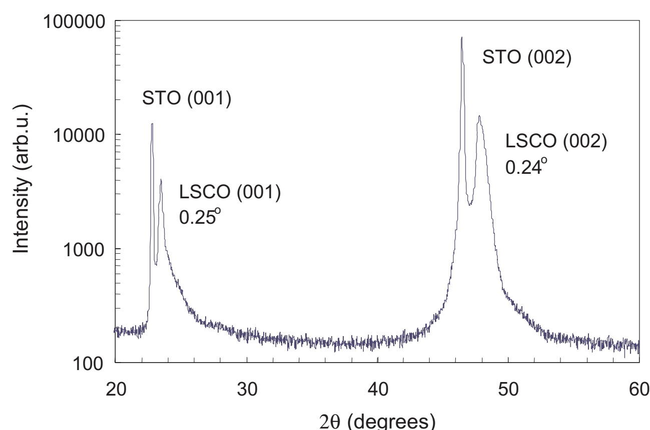

Fig. 3. θ-2θ X-ray diffraction scan of LSCO/$SrTiO_3$ film deposited at 620 °C. Also indicated are the FWHM of the rocking curves of the (001) and (002) LSCO peaks

films exhibit metallic conductivity (Fig. 1) and the film resistivity is typically 100 μΩcm at 300 K. For higher or lower deposition temperatures the films exhibit semiconductivity (i.e. a negative $\mathrm{d}\varrho/\mathrm{d}T$).

Figure 2 shows the surface morphology of a 100 nm thick LSCO/$SrTiO_3$ film deposited at 620 °C. Since the observed Reflected High-Energy Electron Diffraction (RHEED) data during the growth of LSCO imply a step-flow growth mode, the characteristic straight terrace ledges of the single terminated $SrTiO_3$ surface are still just visible. Consequently, films are atomically smooth, with a typical r.m.s. roughness of only 1–2 Å for 100 nm thick films.

X-ray diffraction analysis of a 50 nm thick epitaxial LSCO/$SrTiO_3$ film revealed that films deposited at 620 °C are fully (001) oriented since there are no reflections originating from the (110) or (111) orientations (Fig. 3). The measured full width at half-maximum (FWHM) of the rocking curves of the (001) and (002) film peaks were 0.25° and 0.24°, respectively, which indicates a low mosaic spread. The out-of-plane lattice parameter is 3.79 Å, whereas the lattice parameter of the LSCO target equals 3.84 Å. Hence the film exhibits in-plane tensile strain caused by the lattice mismatch with the substrate (1.7% at room temperature). As a result, the out-of-plane lattice parameter is lowered due to elastic deformation of the film. It is important that a low cooling rate (5 °C min^{-1}) is employed, since the misfit between the film and the substrate increases during cooling, caused by the difference in thermal expansion coefficients between the film and the substrate. Higher cooling rates lead to the formation of micro-cracks along the crystal axes that relieve the misfit. As a consequence, a pattern of regularly aligned rectangular blocks is formed on the surface [4]. The micro-cracks are unwanted for device applications, since they cause a deterioration in the electrical properties of the film.

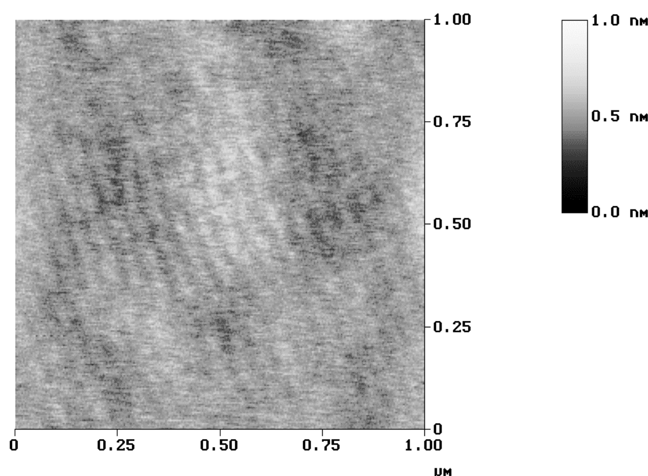

Fig. 2. Atomic force micrograph of a 100 nm thick LSCO/$SrTiO_3$ film

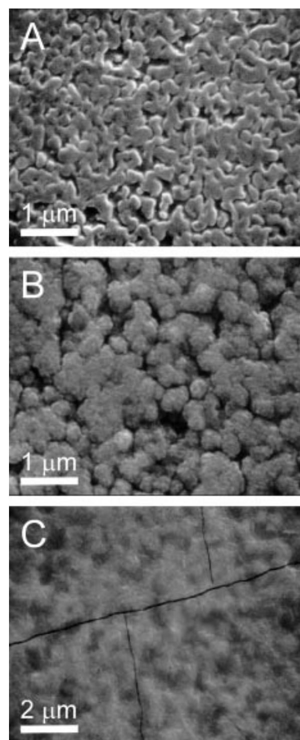

Fig. 4a–c. Scanning electron micrograph of **a** a macroporous α-Al_2O_3 substrate, **b** a 600 nm thick LSCO/α-Al_2O_3 film deposited at 0.1 mbar oxygen pressure, and **c** a 800 nm thick LSCO/α-Al_2O_3 film deposited at 10^{-2} mbar oxygen pressure. The deposition temperature was 650 °C for both films

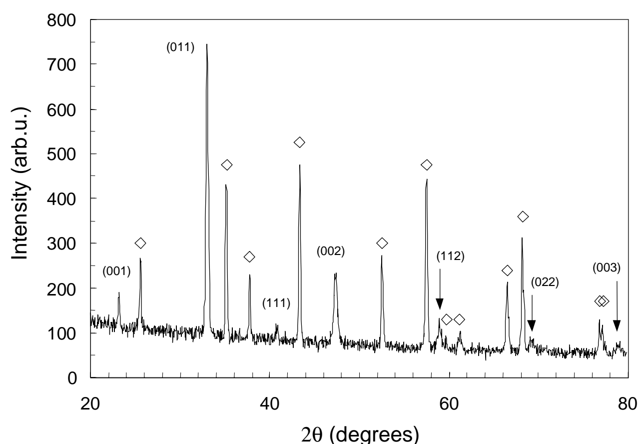

Fig. 5. θ-2θ X-ray diffraction scan of an LSCO/α-Al_2O_3 film deposited at 650 °C in an oxygen pressure of 10^{-2} mbar. The Bragg diffractions of the substrate are marked '◇'. The lattice parameter is 3.84 Å

LSCO films, 500–1000 nm thick, were deposited on the porous α-Al_2O_3 substrates. The substrate temperature of the α-Al_2O_3 substrates was varied from 500 to 800 °C and the oxygen pressure was varied from 10^{-1} to 10^{-2} mbar. The target-to-substrate distance was kept constant at the value optimized for growth on $SrTiO_3$, namely 63 mm. The laser repetition frequency was 10 Hz. The film resistivity was lowest for films grown at temperatures between 600 and 700 °C. In contrast to the (001) textured LSCO/$SrTiO_3$ films, the temperature dependence of the resistivity showed a semiconductive behavior for all deposition temperatures. Figure 1 shows the resistivity of a LSCO/α-Al_2O_3 film deposited at the optimal growth temperature. Films deposited at this temperature exhibit a room temperature resistivity that is about 20 times larger than the room temperature resistivity of epitaxial LSCO/$SrTiO_3$ films deposited at the optimal growth temperature. The oxygen pressure during deposition was not critical with respect to the electrical conductivity of the films.

Figure 4a shows the surface morphology of a polished α-Al_2O_3 substrate. Although the mean substrate pore diameter is 80 nm, pores with much larger sizes can be observed. The typical morphology of a 600 nm thick LSCO/α-Al_2O_3 film deposited at 650 °C and an oxygen pressure of 10^{-1} mbar is presented in Fig. 4b. The LSCO film is macroporous and is composed of large faceted grains of about 300–500 nm in size. Increasing the film thickness up to 1000 nm does not decrease the film porosity. However, lowering the oxygen pressure to 10^{-2} mbar leads to a drastic change in film morphology (Fig. 4c). At reduced oxygen pressures, relatively smooth (with r.m.s. values of 6–9 nm) and dense films are obtained that completely cover the substrate pores. Unfortunately, a strong strain is induced in the film during cooling, caused by different thermal expansion coefficients. As a result, films crack during cooling despite the slow cooling rate of 5 °C min^{-1}. Cracking might be avoided by applying a film material with a lower thermal expansion coefficient or by using perovskite substrates.

LSCO and α-Al_2O_3 differ from each other in lattice parameters and crystal structure (cubic vs. corundum). In addition, the substrate roughness is large because of the large open pores. Nevertheless, the deposited films exhibit good crystallinity and do not contain impurity phases, as can be observed in Fig. 5. Since there is no epitaxial relationship between the film and the substrate surface, the films are polycrystalline. Therefore the films contain many grain boundaries, which give rise to the semiconducting behavior.

The observed change in growth mode is related to the distance over which the plasma thermalizes. Lowering the oxygen pressure rapidly increases the thermalization distance of the plasma, with the consequence that, at constant target-to-substrate distance, atoms arrive at the substrate surface with much larger energy [14]. A detailed investigation of the growth mechanism on porous substrates is currently under way.

3 Conclusions

High-quality (001) textured LSCO thin films have been prepared on TiO_2-terminated $SrTiO_3$ substrate surfaces by pulsed laser deposition. Films grow pseudomorphically and exhibit a very low roughness. Applying a slow cooling rate prevents the film from cracking during cooling caused by thermal stress. Polycrystalline LSCO films were prepared on macroporous polycrystalline α-Al_2O_3 substrates. The oxygen pressure during deposition greatly influences the resulting film morphology. Aside from the observation that films deposited on α-Al_2O_3 can crack due to thermal stress, it has been demonstrated that, at reduced oxygen pressures, the films deposited can completely cover the large substrate pores. This has technological implications for utilizing pulsed laser deposition for new applications and illustrates the versatility of the pulsed laser deposition technique.

Acknowledgements. The authors thank the Dutch technology foundation STW (Stichting Technische Wetenschappen) for financial support. Natascha Sibelt is acknowledged for the preparation of the targets and substrates.

References

1. J.T. Cheung, P.E.D. Morgan, D.H. Lowndes, X-Y. Zheng, J. Breen: Appl. Phys. Lett. **62**, 2045 (1993)
2. C.-S. Hou, C.-C. Chou, H-F. Cheng: Appl. Surf. Sci. **113-114**, 207 (1997)
3. K.W. Wong, W. Wu, P.W. Chan, J.T. Cheung: Thin Solid Films **312**, 7 (1998)
4. M. Li, Z.-L. Wang, S. Fan, Q.-T. Zhao, G. Xiong: Thin Solid Films **323**, 304 (1998)
5. P.W. Chan, W. Wu, K.H. Wong, K.Y. Tong, J.T. Cheung: J. Phys. D: Appl. Phys. **30**, 957 (1997)
6. X. Chen, N.J. Wu, D.L. Ritums, A. Ignatiev: Thin Solid Films **342**, 61 (1999)
7. X. Chen, N.J. Wu, A. Ignatiev: J. Eur. Cer. Soc. **19**, 819 (1999)
8. L.G. Coccia, G.C. Tyrrell, J.A. Kilner, D. Walner, R.J. Chater, I.W. Boyd: Appl. Surf. Sci. **96-98**, 795 (1996)
9. Y. Teraoka, T. Fukuda, N. Miura, N. Yamazoe: J. Ceram. Soc. Jpn. Inter. Ed. **97**, 523 (1989)
10. M. Liu, D. Wang: J. Mater. Res. **10**, 3210 (1995)
11. C. Xia, T.L. Ward, P. Atanasova, R.W. Schwartz: J. Mater. Res. **13**, 173 (1997)
12. E.A.F. Span, F.J.G. Roesthuis, D.H.A. Blank, H. Rogalla: Appl. Surf. Sci. **150**, 171 (1999)
13. G. Koster, B.L. Kropman, G.J.H.M. Rijnders, D.H.A. Blank, H. Rogalla: Appl. Phys. Lett. **73**, 2920 (1998)
14. M. Strikovski, J.H. Miller, Jr: Appl. Phys. Lett. **73**, 1733 (1998)